European Journal of Pharmaceutics and Biopharmaceutics 170 (2022) 59–69

Contents lists available at ScienceDirect

European Journal of Pharmaceutics and Biopharmaceutics

journal homepage: www.elsevier.com/locate/ejpb

Influence of short term storage conditions, concentration methods and excipients on extracellular vesicle recovery and function

S.I. van de Wakker [a], J. van Oudheusden [a], E.A. Mol [a], M.T. Roefs [a], W. Zheng [b], A. Görgens [b], S. El Andaloussi [b], J.P.G. Sluijter [a,1], P. Vader [a,c,1,*]

[a] Department of Cardiology, Experimental Cardiology Laboratory, University Medical Center Utrecht, Utrecht University, the Netherlands
[b] Department of Laboratory Medicine, Clinical Research Center, Karolinska Institutet, Stockholm, Sweden
[c] CDL Research, University Medical Center Utrecht, the Netherlands

ARTICLE INFO

Keywords:
Extracellular vesicles
Recovery
Regenerative medicine
Isolation process
Function

ABSTRACT

Extracellular vesicles (EVs) are phospholipid bilayer enclosed vesicles which play an important role in intercellular communication. To date, many studies have focused on therapeutic application of EVs. However, to progress EV applications faster towards the clinic, more information about the physical stability and scalable production of EVs is needed. The goal of this study was to evaluate EV recovery and function after varying several conditions in the isolation process or during storage.

Physical stability and recovery rates of EVs were evaluated by measuring EV size, particle and protein yields using nanoparticle tracking analysis, microBCA protein quantification assay and transmission electron microscopy. Western blot analyses of specific EV markers were performed to determine EV yields and purity. EV functionality was tested in an endothelial cell wound healing assay.

Higher EV recovery rates were found when using HEPES buffered saline (HBS) as buffer compared to phosphate buffered saline (PBS) during EV isolation. When concentrating EVs, 15 ml spinfilters with a 10 kDa membrane cutoff gave the highest EV recovery. Next, EV storage in polypropylene tubes was shown to be superior compared to glass tubes. The use of protective excipients during EV storage, i.e. bovine serum albumin (BSA) and Tween 20, improved EV preservation without influencing their functionality. Finally, it was shown that both 4 °C and −80 °C are suitable for short term storage of EVs. Together, our results indicate that optimizing buffer compositions, concentrating steps, protective excipients and storage properties may collectively increase EV recovery rates significantly while preserving their functional properties, which accelerates translation of EV-based therapeutics towards clinical application.

1. Introduction

Extracellular vesicles (EVs) are nano-sized endogenous vesicles that are secreted by all cells. They play an important role in intercellular communication through transfer of their biological cargo, including proteins, lipids, RNA, and metabolites [1]. EVs are a heterogeneous group of vesicles that are roughly between 30 and 1000 nm in size and are often categorized in three populations based on their size and mode of secretion. These populations include apoptotic bodies, ectosomes (or microvesicles) and exosomes [1–3].

Being part of the intercellular communication machinery, EVs can influence the cellular microenvironment and mediate both physiological and pathological processes. These combined properties make EVs an interesting source for a wide variability of clinical applications [4]. As a result, research into EV applications has grown exponentially. Carrying specific cargo derived from their parental cells, and being readily accessible in many body fluids, EVs and their associated cargo are considered promising candidate biomarkers [5]. In addition, EVs may be applied as drug delivery vehicles [6]. As natural transporters of proteins and different species of RNA, EVs have attractive characteristics that may be employed for efficient drug transport [7]. In fact, safe usage of EVs has been shown in early clinical trials [8,9]. Furthermore, EVs derived from stem cells are being studied for their regenerative capacities and have shown to promote tissue repair and regeneration in

* Corresponding authors at: CDL Research, University Medical Center Utrecht, Utrecht 3584CX, The Netherlands.
E-mail address: pvader@umcutrecht.nl (P. Vader).
[1] equal contributions

https://doi.org/10.1016/j.ejpb.2021.11.012
Received 30 July 2021; Received in revised form 16 November 2021; Accepted 25 November 2021
Available online 2 December 2021

various animal models [10–12], including cardiac repair and rejuvenation [3,13]. Among other EV types, the use of cardiac progenitor cell (CPC)-derived EVs has shown potential to induce cardiac regeneration through stimulation of angiogenesis and cell proliferation [14,15].

In order to successfully use EVs as a therapeutic, a scalable source of well-characterized EVs is required. However, obtaining high EV yields using current isolation techniques remains challenging. Upscaling EV production is the most obvious solution to increase EV yields, but optimization of the subsequent isolation procedure while ensuring physical stability of EVs could significantly contribute to recover higher EV yields. Therefore, increased knowledge on the physical stability as well as on factors influencing EV recovery is warranted.

During the isolation procedure, EVs can aggregate or stick to membranes, column resin or other surface areas by adhesion, resulting in EV loss [16,17]. However, surprisingly little is known about how these physical stability properties of EVs influence their recovery during the isolation process and storage. Moreover, there is no consensus on which materials or which temperatures are optimal for EV storage. The goal of the current study was to evaluate EV recovery and functionality in a systematic manner after varying different steps and conditions in the isolation and storage process, including choice of buffers, concentration methods, storage tubes, protective excipients, and storage temperatures.

2. Materials and methods

2.1. Cell culture

Cardiac progenitor cells (CPCs) were obtained as previously described [18]. CPCs were cultivated in MEM 199 + Earle's Salts and L-glutamine (Life Technologies) which was supplemented with 22% EGM-2 medium (Lonza), 1% penicillin/streptomycin (Gibco), 10% fetal bovine serum (FBS) and 1% MEM NEAA Nucleic acids (Gibco). Human Microvascular Endothelial Cells-1 (HMEC-1) were cultured in MCDB-131 medium (Life Technologies) supplemented with 10% FBS, 1% GlutaMAX (Gibco), 1% penicillin/streptomycin, 10 ng/ml rhEGF (Peprotech) and 50 nM Hydrocortisone (Sigma). All cells were cultured at 37 °C and 5% CO_2 in flasks or plates coated with 0.1% gelatin (Sigma).

2.2. Isolation of CPC-derived EVs

When a confluency of 80–90% was reached, CPCs were washed with PBS and medium was replaced for plain (FBS-free) MEM199 medium. Conditioned medium was removed after 24 h and spun down for 15 min at 2000 × *g*. Supernatant was filtered through a 0.45 μm aPES bottle top filter (Nalgene). Filtrate was concentrated to a volume of approx. 3 ml by Tangential Flow Filtration (TFF) using a Minimate TFF capsule with a membrane cutoff of 100 kDa. During TFF, a buffer exchange was performed to the appropriate buffer (i.e. PBS, unless indicated otherwise). The residue was loaded on a HiScreen Capto Core 700 column (GE Healthcare) connected to an ÄKTA start system (GE Healthcare). An absorbance chromatogram was recorded at 280 nm. EV-containing fractions were pooled and concentrated using 100 kDa Amicon Ultra-15 spinfilters (Merck) and stored in PBS unless indicated otherwise. A schematic overview of the isolation protocol is shown in Fig. 1A.

HBS buffer contained 25 mM HEPES (441476L, VWR Chemicals) and 0.9% Sodium Chloride (31434, Sigma-Aldrich). For storage experiments, EVs were stored at 4 °C or −80 °C in regular polypropylene tubes (VWR, 525–1164), DNA LoBind tubes (Eppendorf, 022431021), low protein binding tubes (Thermo scientific, 90410), 8 ml glass tubes (Qiagen) and 8 ml glass tubes coated with Sigmacote® (Sigma, SL2-100ML) according to the manufacturer's protocol. Additionally, EVs were stored in PBS containing 0.005% Tween 20 (Fisher Bioreagents, 9005–64-5), or containing 0.1% or 0.2% bovine serum albumin (BSA) (Roche, 10735086001). To compare yields, we calculated recoveries defined as the number of particles/amount of protein in the output material divided by the number of particles/amount of protein in the stock *100%.

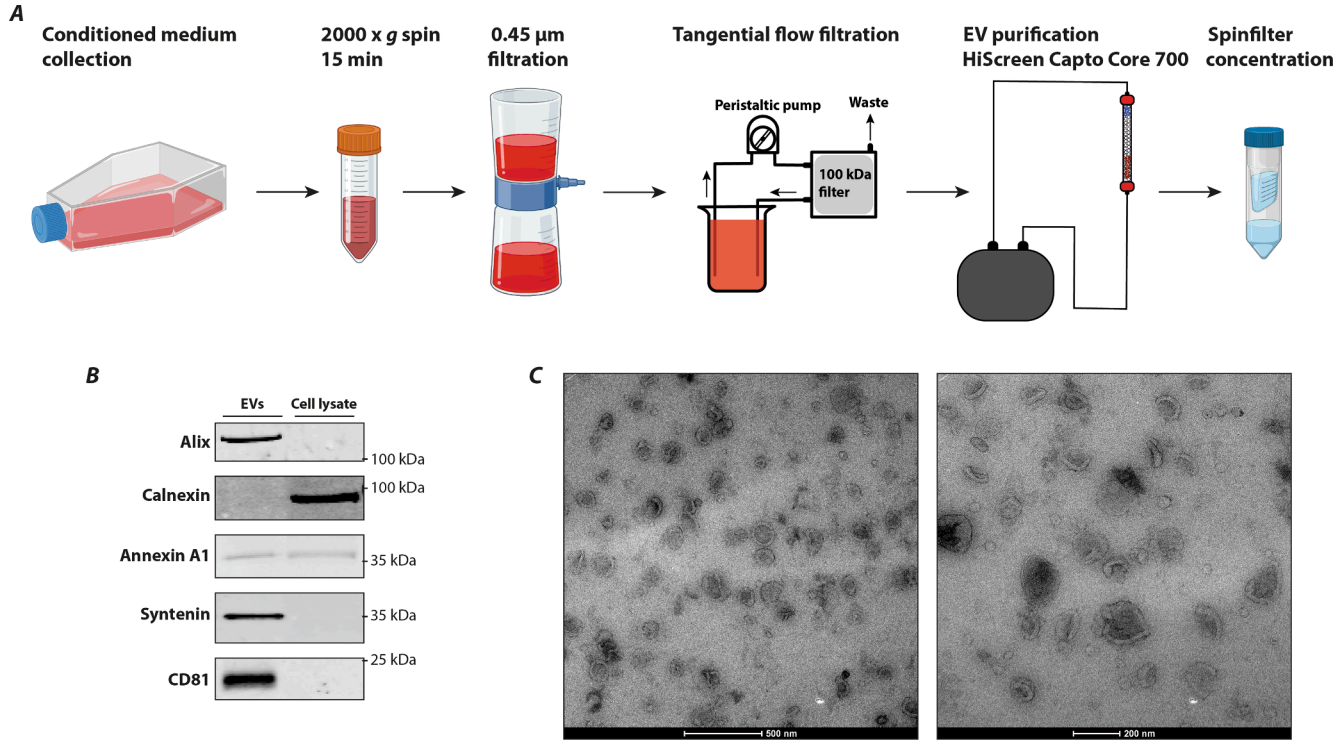

Fig. 1. Characterization of EVs. A: Schematic overview of the EV isolation procedure. **B:** Western blot analysis of CPC-derived EVs and their host cell lysate. Equal protein amounts (5 μg) were loaded. **C:** TEM pictures of purified EVs (size bars: 500 and 200 nm).

2.3. PEG precipitation

Purified EVs were equally split in two fractions. One fraction was concentrated using a 15 ml 10 kDa spinfilter while the other fraction was concentrated using PEG precipitation [17]. Briefly, a purified EV sample was mixed 1:1 (v/v) with a PEG solution containing 20% PEG 6000, 200 mM NaCl, 10 mM EDTA, 200 mM Tris-HCl, pH 7.0. The mixture was incubated overnight on a roller bench at 4 °C and the next day centrifuged for 15 min at 4000 × *g*.

2.4. Western blot analysis

For SDS PAGE (sodium dodecyl sulphate polyacrylamide gel electrophoresis), samples were diluted with LDS sample buffer (Life Technologies) containing sample reducing agent (Life Technology). Subsequently, samples were heated for 10 min at 95 °C and were separated on a 4–12 Bis-Tris polyacrylamide gel (Thermo Scientific) next to a PageRuler Plus Prestained Protein Ladder (ThermoFisher Scientific). During blotting, samples were transferred from the gel to a nitrocellulose iBlot membrane (iBlot 2 NC mini Stacks, Invitrogen) with the iBlot 2 apparatus (Life Technologies). Membranes was blocked for 1 h in 50% v/v Intercept Blocking Buffer (LI-COR Biosciences) in Tris buffered saline (TBS). All immune-labeling was performed with 50% v/v Intercept Blocking Buffer and TBS containing 0.1% Tween 20 (TBS-T) for 2 h at room temperature or overnight at 4 °C. Primary antibodies included mouse anti-Alix (Thermo Scientific, MA1-83977, 1:1000 dilution), mouse anti-syntenin (Origene, TA504796, 1:1000 dilution), mouse anti-CD81 (Santa Cruz, SC-166029; 1:1000), rabbit anti-Annexin A1 (Abcam, ab214486, 1:1000 dilution), rabbit anti-calnexin (GeneTex, GTX 101676, 1:1000 dilution), mouse anti-β-actin (Cell Signaling Technology, clone 8H10D10, 1:1000 dilution). Secondary antibodies included Alexa Fluor 680-conjugated anti-mouse antibody (LI-COR Biosciences, A-21057; 1:10,000 dilution) and IRDye 800CW anti-rabbit antibody (LI-COR Biosciences, 926–32211, 1:7500 dilution). Imaging was performed on an Odyssey Infrared Imager (LI-COR Biosciences) at 700 nm and 800 nm.

For preparation of CPC cell lysates, cells were collected in trypsin and centrifuged at 400 × *g* for 10 min. Cells were washed with PBS and collected in 1 ml complete lysis-M Reagent (Roche) supplemented with protease inhibitor and phosphatase inhibitors. After incubation on ice for 30 min the solution was centrifuged for 10 min at 12,000 × *g* at 4 °C. Supernatant was stored at −20 °C.

2.5. Silverstain analysis

SDS PAGE was performed as described under Western blot analysis. A Silverstain assay was performed according to manufacturer 's instructions for protein detection (Thermo Scientific™ Pierce™ Silver Stain Kit, ThermoFisher Scientific, 10096113). Imaging was performed on a ChemiDoc MP Universal Hood III imaging system (Bio-Rad).

2.6. Endothelial cell wound healing assay

HMEC-1 were seeded in a 48-well plate at a density of 90,000 cells/well 48 h prior to the assay. A scratch wound was made using a pipet tip and detached cells were washed away with basal MCDB-131 medium. Subsequently, cells were incubated in basal MCDB-131 medium plus indicated treatments in triplicate for 6 h. For the EV samples, 3 μg per well was added. PBS was used as a negative control and MCDB-131 containing 20% FBS as a positive control. At t = 0 h and t = 6 h, two pictures per well were taken using an EVOS microscope (Life Technologies). Closing of the scratch was measured by image analysis using Image J software. The mean width of each scratch at t = 0 h was subtracted by the mean width at t = 6 h to determine the migrated distance. Relative wound closure was calculated relative to the negative control.

2.7. Micro bicinchoninic acid assay (BCA) analysis

A BCA assay was performed according to manufacturer 's instructions to measure total protein concentrations (MicroBCA™ Protein Kit , Life Technologies, 23235). Absorbance was determined using a Multiskan™ FC Microplate Photometer (ThermoFisher Scientific).

2.8. Nanoparticle tracking analysis

Particle size and concentration was determined with a Nanosight NS500 nanoparticle analyzer using NanoSight NTA 3.3 software. Three videos of 30 s were recorded for each sample with a delay of 5 s between each video. For all the recordings, the camera level was set at 16 with a well-adjusted camera focus. Detection threshold was set at 5, screen gain at 1.0 while other functions were set to automatic. Samples were diluted in PBS.

2.9. Imaging flow cytometry

EVs were studied on a single EV level by high resolution IFCM (Amnis Cellstream, Luminex; equipped with 405, 488, 561 and 642 nm lasers) based on previously optimized settings and protocols with an Amnis ImagestreamX MkII instrument [19]. Briefly, fluorescence-conjugated antibodies were used to stain for EV surface markers. Antibodies were added to EV-containing samples diluted to a concentration of 1×10^{10} particles/mL at a final concentration of 8 nM, and samples were incubated over-night at room temperature. All antibodies were centrifuged for 10 min at 17,000 × *g* before they were applied to EV samples. The following antibodies were used: CD9-APC (Miltenyi Biotech, clone SN4), CD63-APC (Miltenyi Biotec, clone H5C6), and CD81-APC (Beckman Coulter, clone JS64). Post staining, samples were diluted 2000 fold in PBS before acquisition by using the plate reader of the Cellstream instrument with FSC turned off, SSC laser set to 40%, and all other lasers set to 100% of the maximum power. EVs were defined as SSC (low) by using neonGFP-tagged EVs as biological reference material and regions to quantify APC + positive events were set according to unstained samples and unstained neonGFP-tagged reference control EVs as described before [19]. Samples were acquired for 5 min at a flow rate of 3.66 μl/min (setting: slow) with CellStream software version 1.2.3 and analyzed with FlowJo Software version 10.5.0 (FlowJo, LLC). Dulbecco's PBS pH 7.4 (Gibco) was used as sheath fluid.

2.10. Transmission electron microscopy (TEM)

Isolated EVs were pelleted using ultracentrifugation at 100,000 × *g* for 60 min at 4 °C using a type 50.2 Ti fixed-angle rotor and resuspended in PBS. Subsequently, EVs were adsorbed to carbon-coated formvar grids for 15 min at room temperature. After a PBS wash, the grids were fixed in a 2% paraformaldehyde, 0.2% glutaraldehyde in PBS fixing buffer for 30 min at room temperature, followed by counterstaining with uranyl-oxalate. Grids were embedded in a mixture of 1.8% methyl cellulose and 0.4% uranyl acetate at 4 °C and imaged on a Jeol JEM-1011 TEM microscope (Jeol).

2.11. Statistics

Statistical analyses were performed using Prism 5.0 (GraphPad Software Inc.). Differences between two groups were tested with a paired or unpaired *T*-test. An one sample *t*-test was performed to determine significance between relative comparisons. Comparisons of more than two groups were tested with one-way ANOVA followed by Tukey's HSD multiple comparison test as post-test. Comparisons of more than two groups affected by two factors were tested with two-way ANOVA followed by Bonferroni as post-test. Differences with p-values < 0.05 were considered statistically significant. All results are expressed as mean ± standard deviation.

3. Results

In this study, EV recovery and functionality were evaluated after varying different steps and conditions in the isolation and storage process. In Fig. 1A, an overview of our initial isolation procedure is shown. Briefly, EVs were isolated from conditioned medium of CPCs. After centrifugation and filtering steps, conditioned medium was concentrated with TFF before injecting the residue into a HiScreen 700 Capto Core column to purify EVs. After elution, EVs were concentrated using spinfilters of 15 ml with a membrane cutoff of 100 kDa. PBS was used as mobile phase for chromatography and as a storage buffer. All EVs were stored at 4 °C in regular polypropylene tubes.

According to international EV research guidelines, MISEV2018 [20], protein characterization was done for CPC-derived EVs compared to their host cells. Enrichment of EV protein marker expression compared to their host cells was shown for alix, syntenin and CD81, while the endoplasmic reticulum marker calnexin was, as expected, only detected in cell lysate (Fig. 1B). Annexin A1 was similarly expressed in EVs and their host cells. EV morphology was assessed with TEM, showing bilayer-enclosed vesicles in a size range of 30–200 nm (Fig. 1C).

3.1. EV isolation using HBS as mobile phase and storage buffer increases EV recovery compared to PBS

PBS is the most widely used buffer for EV storage and as a mobile phase during chromatography for EV purification. Buffers containing phosphate, however, are known to show pH shifts with concentration changes or upon freezing, which may lead to aggregation and/or loss of enzymatic activity [21–23]. Furthermore, phosphate precipitates in presence of high concentrations of metal ions, such as calcium, which impacts the buffering capacity [24]. For this reason, we explored if HBS, which does not show this behavior, would be an appropriate alternative buffer for EV isolation. To determine influence on EV recovery, HBS or PBS were used for buffer exchange during TFF, as a mobile phase during the column purification step, and for prewashing of the spinfilters before EV concentrating (Fig. 2A).

Interestingly, when HBS was used instead of PBS at different stages during isolation, a significantly higher particle recovery was found (14% ± 6) (Fig. 2B). Conversely, a slight but not-significant lower protein recovery was observed (Fig. 2C). This resulted in a higher particle/protein ratio for EVs isolated in HBS, which is suggestive of increased purity (Fig. 2D) [25]. The results of the higher particle recovery for HBS samples were confirmed by western blot analysis, revealing higher expression levels of EV marker proteins alix and annexin A1, and to a

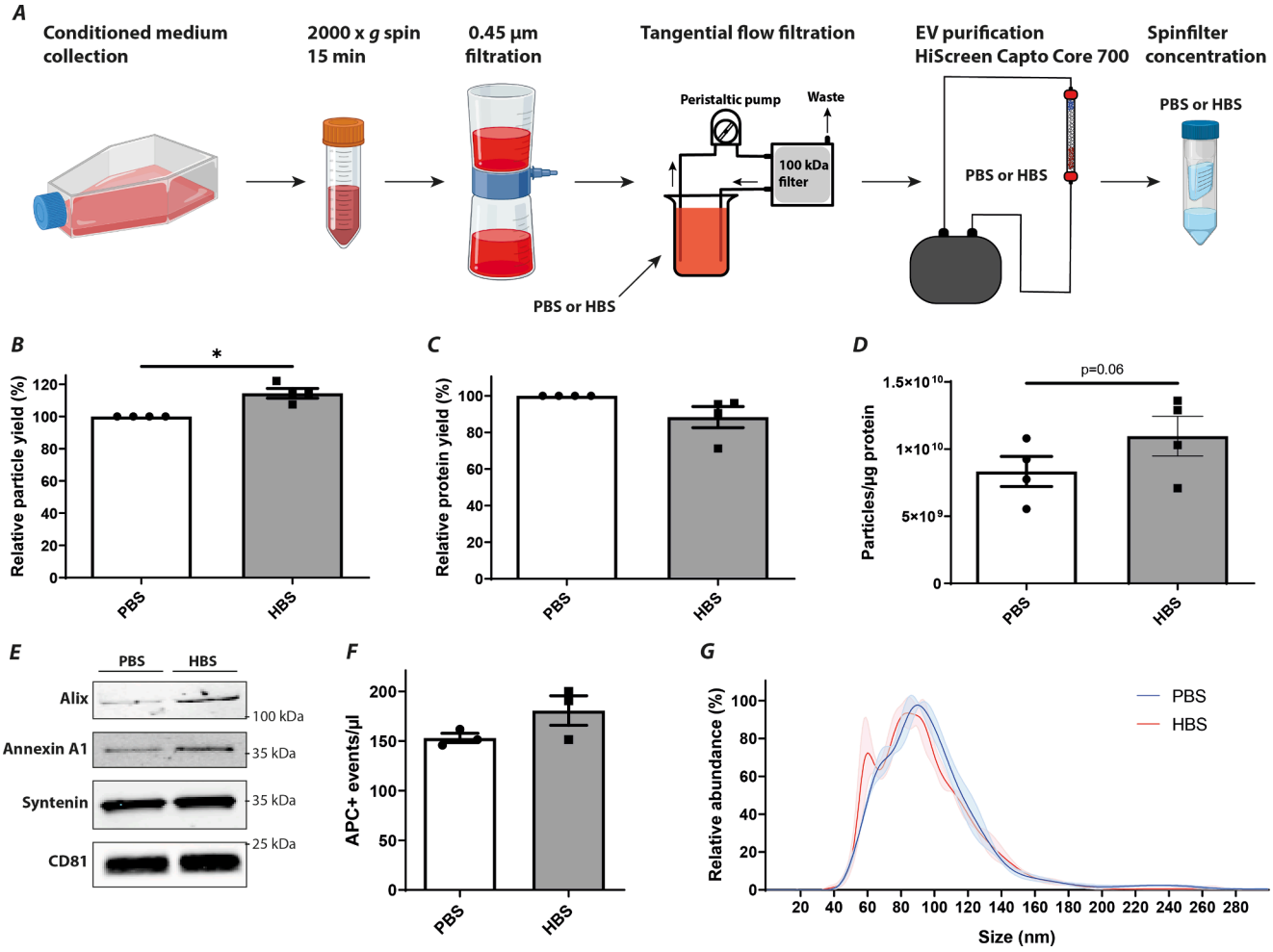

Fig. 2. Characterization of EVs isolated using PBS or HBS buffer. A: Schematic overview of the experimental setup. **B:** Relative particle recovery as determined by NTA (absolute recoveries were for PBS: $4.2E^{11} \pm 2.4E^{11}$particles, for HBS: $4.8E^{11} \pm 2.7E^{11}$ particles). **C:** Relative protein recovery as determined by microBCA protein determination (absolute recoveries were for PBS: 49.9 ± 21.8 µg, for HBS: 44.9 ± 22.1 µg). **D:** Particle/protein ratios of EVs. **E:** Western blot analysis of EV markers CD81, syntenin, alix and Annexin A1. Equal percentages of the total volume of EV isolates were loaded. **F:** Particle quantification of EVs positive for CD9, CD63 or CD81 (labeled with APC-conjugated antibodies) as determined by imaging flow cytometry. **G:** Particle size ranges determined with NTA. Results in B, C and D represent biological replicates (n = 4), results in E and F represent technical replicates (n = 3). Significance levels are indicated with asterisks (* $p < 0.05$).

lesser extent syntenin and CD81 (Fig. 2E). Imaging flow cytometry was used for quantification of tetraspanin positive EVs, after CD9, CD63 and CD81 were labeled with APC-conjugated antibodies. Imaging flow cytometry analysis confirmed our previous results, indicating a non-significant trend towards higher tetraspanin-positive EV count for EVs isolated with HBS (Fig. 2F). Choice of buffer did not impact the size of the isolated EVs (Fig. 2G, S1A and S1B). Thus, using HBS instead of PBS during the isolation procedure resulted in improved EV recovery.

3.2. Concentrating using 15 ml spinfilters with a size cutoff of 10 kDa provides the highest EV recovery

Concentrating EV samples during or after a purification step is often essential for subsequent EV analyses or functional studies. However, it is well recognized that during these concentration steps many EVs are lost because of adhesion, aggregation or destruction. The most widely used method to concentrate EVs is filtration using centrifugal spinfilters. These spinfilters are available with different membrane materials, pore sizes, and volumes. In this study, we compared spinfilters of 4 ml and 15 ml containing regenerated cellulose membranes with pore sizes of 10 or 100 kDa (Fig. 3A). A stock solution of purified EVs was prepared and equal volumes of 4 ml were loaded onto each spinfilter. When analyzing yields before and after EV concentration using the different spinfilters, we observed that overall EV particle and protein recovery efficiencies showed similar trends. Particle recoveries varied between 25 and 70% and protein recoveries between 20 and 50% (Fig. 3B and 3C). Spinfilters with a membrane cutoff of 10 kDa gave significantly higher EV recoveries compared to 100 kDa spinfilters. Surprisingly, 15 ml spinfilters also gave a significantly higher particle recovery compared to the 4 ml spinfilters. Protein recovery displayed a similar trend with a higher recovery rate in the 15 ml spinfilters, however, this difference did not reach significance. As expected, particle/protein ratios were higher for

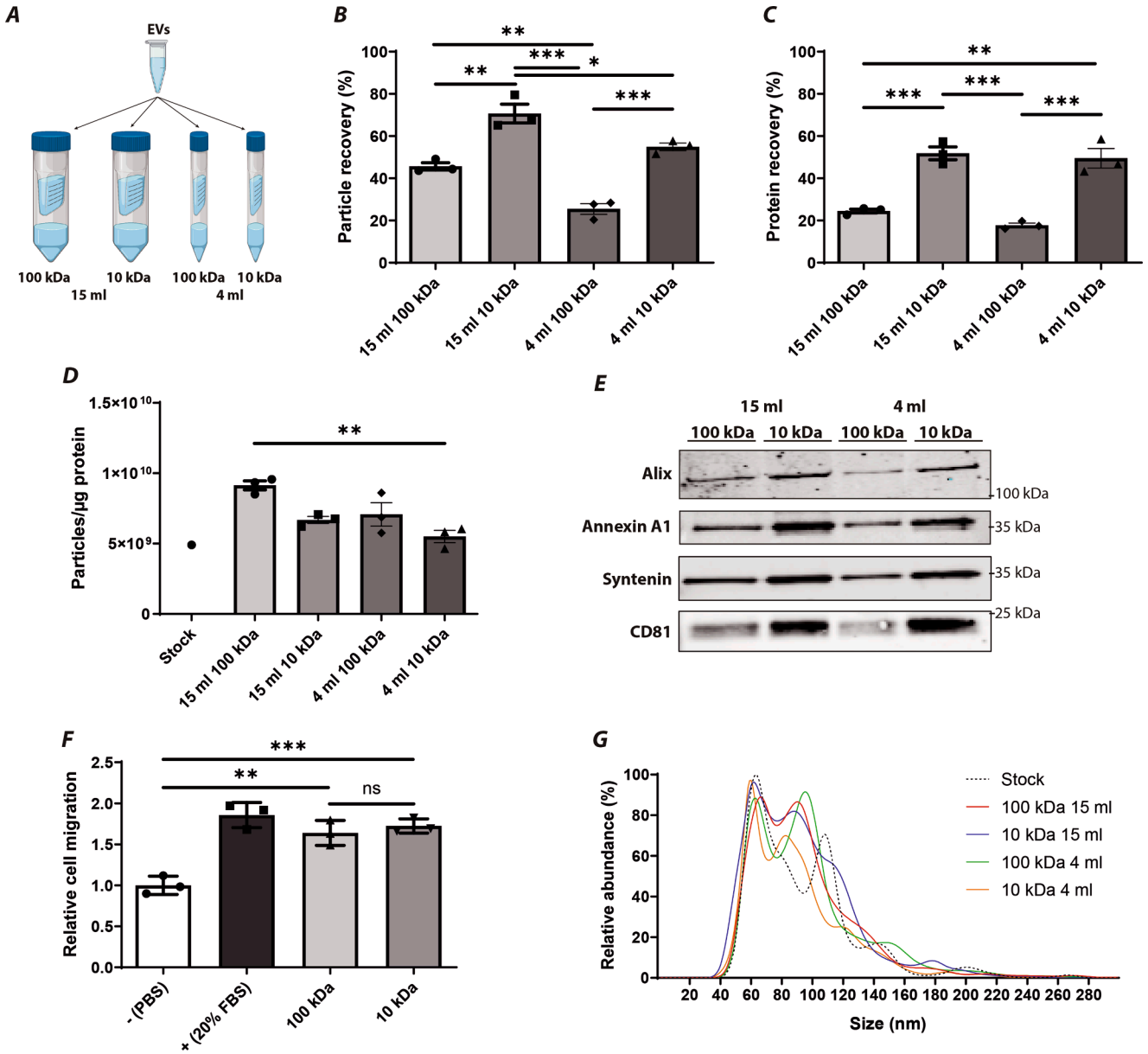

Fig. 3. Effect of spinfilter properties on EV recovery. A: Schematic overview of the experimental setup. **B:** Particle recovery rates as determined by NTA (Stock: $4.2E^{10}$ particles/ml). **C:** Protein recovery rates as determined by microBCA protein determination (Stock: 8.5 µg/ml). **D:** Particle/protein ratios of EVs. **E:** Western blot analysis of EV markers CD81, syntenin, alix and Annexin A1. Equal percentages of the total volume of EV isolates were loaded. **F:** Results of an endothelial cell wound healing assay. **G:** Particle size ranges determined with NTA. Results represent technical replicates (n = 3), and are representative for three independent experiments. Significance levels are indicated with asterisks (* $p < 0.05$, ** $p < 0.01$, *** $p < 0.01$).

spinfilters with a 100 kDa cutoff compared with 10 kDa, since residual proteins > 10 and < 100 kDa are expected to be removed when using 100 kDa spinfilters (Fig. 3D). However, this was not reflected in the EV total protein profile (Figure S2A). Therefore, differences in recovery are more likely to be attributed to general overall loss of protein. To validate differences in recovery, western blot analysis was performed for the abovementioned EV markers (Fig. 3E). For all proteins, a similar trend was observed as shown for the particle and protein recovery, with the highest EV protein expression for the 10 kDa spinfilters. To study the effect of the different spinfilters on EV functionality, we assessed relative HMEC-1 migration after 6 h of treatment with EVs concentrated with 10 or 100 kDa membranes in a wound healing assay (Fig. 3F). Both EVs concentrated with 10 and 100 kDa spinfilters were able to significantly increase endothelial cell migration, and to a similar extent. This indicates that the spinfilter size cut-off does not influence the pro-migratory properties of EVs on endothelial cells. There were no apparent differences in EV size distribution, nor in mean or mode size when concentrated with the different spinfilters (Fig. 3G, S2B-G). In conclusion, for EV concentration, 15 ml spinfilters containing membranes with a pore size cutoff of 10 kDa gave higher EV yields compared to spinfilters with a larger pore size or a smaller volume.

3.3. PEG precipitation for concentrating EVs leads to high losses

Next, we also compared spinfilter concentration to PEG precipitation as an EV concentration method (Fig. 4A). PEG is a polymer that can precipitate proteins and particles based on excluded volume interactions [17]. However, we found that using PEG precipitation, both protein and particle recovery were much lower than using spinfilters (Fig. 4B and 4C). In agreement, western blot analysis showed much higher expression levels of EV marker proteins for the spinfilter concentrated EVs compared to the PEG precipitated EVs (Fig. 4D). Because of these large differences, PEG precipitation of EVs was not further explored.

3.4. Storage in polypropene tubes facilitates higher EV recovery compared to glass tubes

Although it is well recognized that EVs may be partially lost during storage due to nonspecific binding to tubing material, there is little known about the influence of different materials on EV recovery. The most widely used materials are regular hydrophobic polypropene tubes and hydrophilic silicon dioxide glass tubes. Different types of polypropylene tubes are available, each differently treated to reduce adhesion of proteins or nucleic acids. In addition, coatings to shield the hydrophilic characteristics of glass are available, such as Sigmacote. Here we studied whether tube materials and coating influenced EV recovery after short term storage (1 and 7 days) at 4 °C. In general, for particle and protein recovery, similar trends were visible after 1-day storage in the different tube types (Fig. 5A and 5B). This included significantly lower protein recovery for hydrophilic glass tubes compared to other tubes. After 7-days of storage, similar trends were observed, with significantly lower protein recovery for hydrophilic glass tubes as compared to low DNA- and low protein binding tubes (Fig. 5C and 5D). Imaging flow cytometry of tetraspanin positive EVs showed higher counts for all polypropylene tubes compared to hydrophilic and hydrophobic glass tubes after 7 days of storage (Fig. 5E). In addition, EV marker proteins showed similar expression levels between regular-, low DNA binding-, low protein binding- and hydrophobic glass tubes after 7 days of storage, while levels were clearly decreased after storage in hydrophilic glass tubes (Fig. 5F). As expected, no differences in size among EVs stored in different tubes were observed (Figure S3A-G). These results provide evidence that storage in hydrophilic glass tubes may lead to increased EV loss as compared to the other evaluated materials.

3.5. Both *BSA and Tween 20 reduce EV loss during storage*

To protect EVs stored in PBS against aggregation and adhesion, the use of excipients Tween 20 and BSA on EV recovery was explored. Both

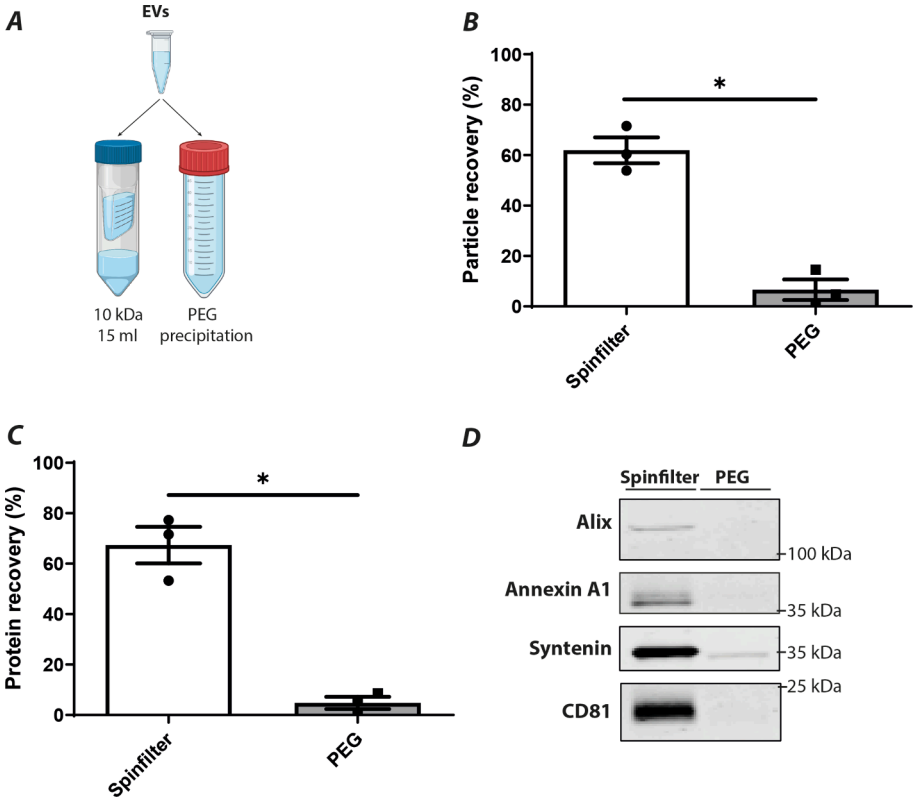

Fig. 4. Effect of spinfilter concentration versus PEG precipitation on EV recovery. A: Schematic overview of the experimental setup. **B:** Particle recovery rates as determined by NTA (Stock: $1.8E^{10} \pm 8.1E^{09}$ particles/ml). **C:** Protein recovery rates as determined by microBCA protein determination (Stock: 39.1 ± 61.7 μg/ml). **D:** Western blot analysis of EV markers CD81, syntenin, alix and Annexin A1. Equal percentages of the total volume of EV isolates were loaded. Results represent biological replicates (n = 3). Significance levels are indicated with asterisks (* $p < 0.05$).

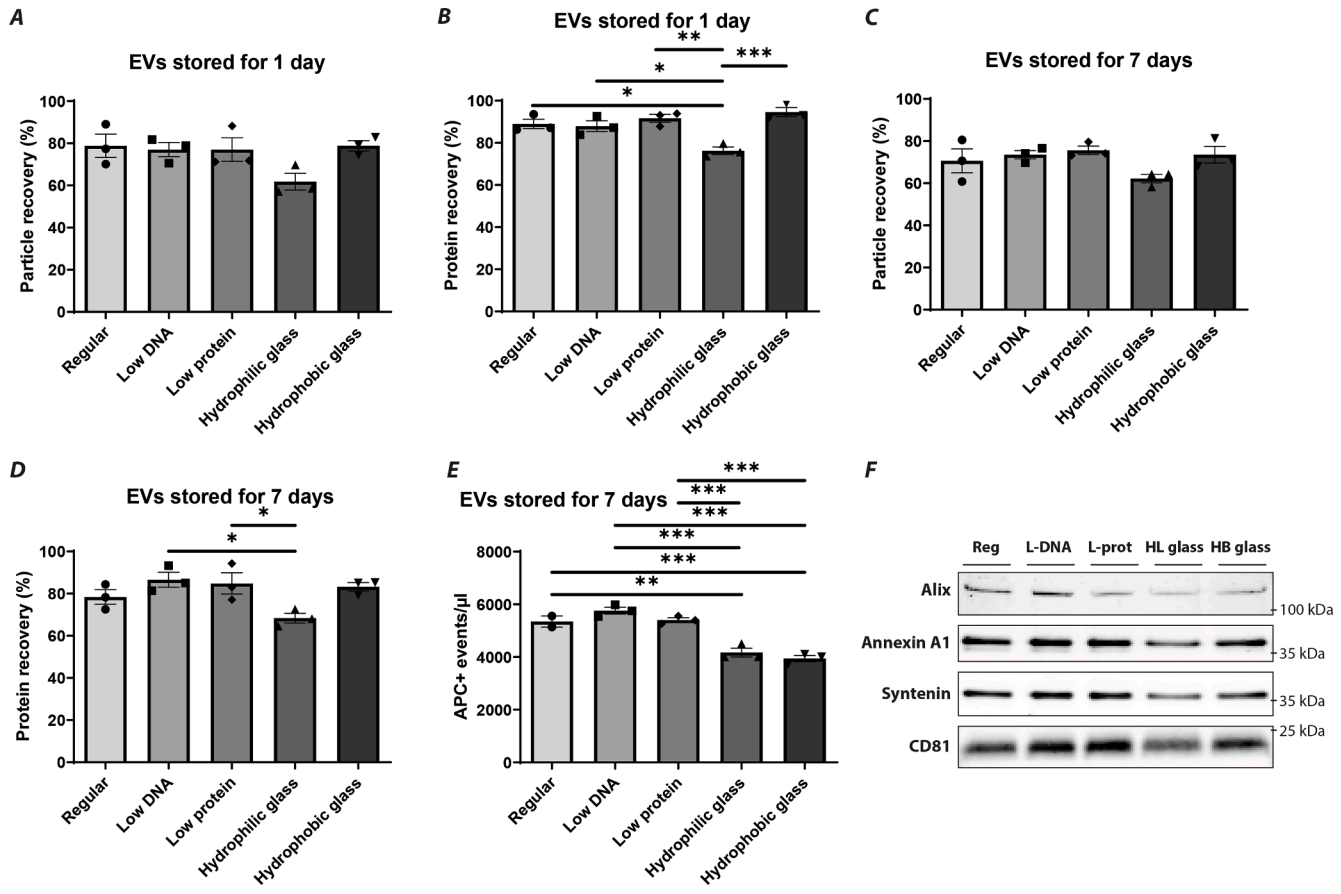

Fig. 5. Effect of different tube materials and coating on EV recovery after storage. A, C: Particle recovery rates as determined by NTA after 1 and 7 days (Stock: $1.2E^{12}$ particles/ml). **B, D:** Protein recovery rates as determined by microBCA protein determination after 1 and 7 days (Stock: 130.5 µg/ml). **E:** Particle quantification of EVs positive for CD9, CD63 or CD81 (labeled with APC) as determined by imaging flow cytometry. **F:** Western blot analysis of EV markers CD81, syntenin, alix and Annexin A1. Equal percentages of the total volume of EV isolates were loaded. Results represent technical replicates (n = 3), and are representative for three independent experiments. Significance levels are indicated with asterisks (* $p < 0.05$, ** $p < 0.01$, *** $p < 0.01$). Reg: regular tubes, L-DNA: low DNA binding tubes, L-prot: low protein binding tubes, HL: hydrophilic, HB: hydrophobic.

Tween 20 and BSA are known to cover solid–liquid interfaces and thereby potentially reduce EV loss because of adhesion. After 1 day of storage, significantly higher particle recoveries were observed when EVs were stored in the presence of 0.005% Tween or 0.2% BSA (Fig. 6A), while Tween also led to higher protein recovery rates (Fig. 6B). Protein recovery rates could not be determined in the presence of high concentrations of BSA. After 7 days of storage, similar patterns on particle and protein recovery were observed (Fig. 6C and 6D), and also Western blot analysis of EVs showed higher expression levels for EV marker proteins when stored in the presence of BSA or Tween (Fig. 6E). Neither Tween nor BSA affected EV size distributions (Figure S4A-F). Next, we evaluated whether BSA or Tween may detrimentally affect EV functionality. Previously, we have shown that CPC-derived EVs have a pro-angiogenic effect *in vitro* and *in vivo* [26,27]. To study the effect of excipients on EVs' functionality, we assessed relative HMEC-1 migration after 6 h of treatment with EVs stored with and without Tween or BSA (Fig. 6E). A significant increase in endothelial cell migration was shown for cells treated with EVs compared to a PBS control, which was not affected by the presence of Tween or BSA. This suggests that Tween nor BSA influenced the pro-migratory properties of EVs on endothelial cells. Thus, both Tween and BSA excipients were able to protect EVs from loss during storage without impacting their function.

3.6. Storage *temperature impacts EV recovery and functionality*

As we move towards employment of EVs for therapeutic use, appropriate storage conditions to maintain EV functionality have to be established. Here, we further evaluated potential storage temperature mediated effects on EV recovery and EV functionality. EVs were stored in PBS and characterized after 1 and 7 days of storage at 4 °C and at −80 °C after which EV functionality was investigated *in vitro*. EVs stored at either 4 °C or −80 °C showed particle recoveries that decreased over time (Fig. 7A). Particle recovery was slightly higher for EVs stored at 4 °C as compared to −80 °C, although this difference did not reach statistical significance. Protein recovery did not differ between storage temperatures (Fig. 7B). In addition, a significant decrease in protein content was observed for both 4 °C and −80 °C stored EVs between 1 and 7 days. Particle/protein ratios of EVs stored at 4 °C were found to be slightly higher compared to −80 °C (Fig. 7C). Western blot analysis for EV markers after 7 days of storage showed no apparent differences in EV marker expression (Fig. 7C). Furthermore, there were no clear differences in size between EVs stored at either temperature (Fig. 7E, S5A, S5B, S5C, S5D). To evaluate potential effects of storage temperature on EV functionality, relative migration of HMEC-1 cells was determined after 6 h treatment with EVs stored at 4 °C or −80 °C for 1 or 7 days (Fig. 7F and 7G). After 1 day of storage, EVs stored at either temperature were able to enhance endothelial cell migration significantly compared to a negative PBS control. Interestingly, a slightly greater effect on migration was shown for EVs stored at 4 °C compared to EVs stored at −80 °C. After 7 days of storage at either temperature, EVs retained the ability to significantly induce endothelial cell migration compared to control. However, in contrast to the migration assay results after 1 day of storage, EVs stored at −80 °C for 7 days had a slightly stronger effect on migration compared to 4 °C stored EVs. It is therefore tempting to

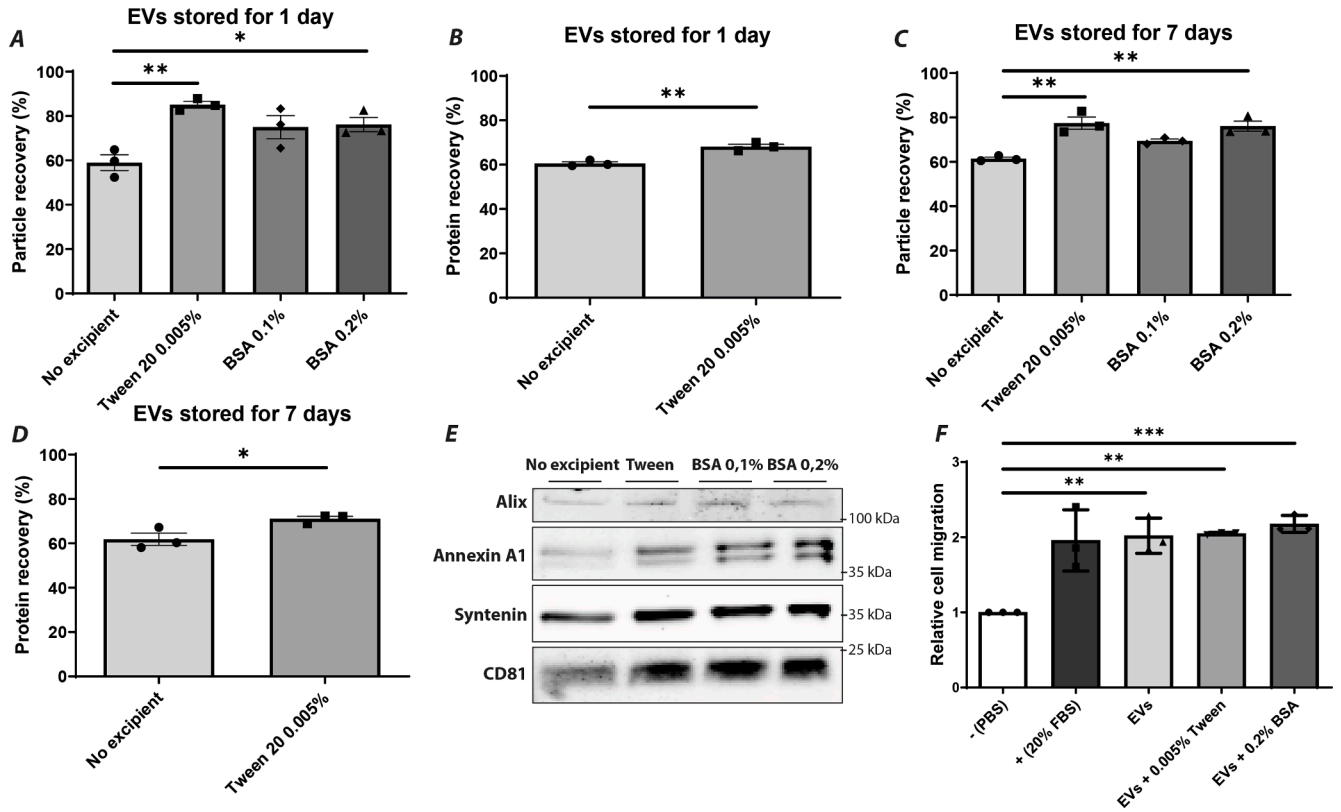

Fig. 6. Effect of Tween 20 and BSA on EV recovery after storage. A, C: Particle recovery rates as determined by NTA after 1 and 7 days (Stock: $1.1E^{12}$ particles/ml). **B, D:** Protein recovery rates as determined by microBCA protein determination after 1 and 7 days (Stock: 197.8 μg/ml). **E:** Western blot analysis of EV markers CD81, syntenin, alix and Annexin A1. Equal percentages of the total volume of EV isolates were loaded. **F:** Results of an endothelial cell wound healing assay performed in the presence of different excipients. Results represent biological replicates (n = 3). Significance levels are indicated with asterisks (* $p < 0.05$, ** $p < 0.01$, *** $p < 0.01$).

conclude that for periods longer than a week, −80 °C storage may be better suited to retain EV functionality.

4. Discussion

EVs are endogenous messengers that have been implicated to contribute to various physiological and pathological processes. Therefore, EVs are increasingly being studied for both therapeutic and diagnostic purposes. Recovery of sufficient yields of EVs remains challenging as a result of adhesion, aggregation or destruction/decomposition [28]. For this reason, optimization of each step in the downstream isolation process and storage conditions is pivotal. The goal of this study was to evaluate EV recovery and function after varying various conditions in the isolation process or during storage. In Table 1, a comparison of recovery rates between the conditions that yielded highest and lowest recovery for all studied conditions is shown.

Although PBS is the most commonly used buffer for EV isolations and storage, we observed that by using HBS instead of PBS as buffer during isolation, a significantly higher particle recovery was found and a lower, but not significant, protein recovery (Table 1), in turn leading to a higher particle/protein ratio. Together with increased abundance of EV protein markers, this suggests the preferable use of HBS over PBS to be used during the isolation process.

In many published isolation procedures, spinfilters have been used to concentrate EVs for functional evaluation at the known expense of EV loss as a result of nonspecific binding to filter materials [29,30]. Spinfilters with regenerated cellulose membranes were previously found to be best suited for EV concentration, being least adhesive as compared to spinfilters with membranes of hydrosart, polyethersulfone and cellulose triacetate [30]. Therefore, we focused here on regenerative cellulose membrane spinfilters only. In our hands, 15 ml 10 kDa spinfilter had highest recovery rates of 71% (±7.7) of particles and 52% (±5.3) of proteins, while 4 ml 100 kDa spinfilters yielded highest EV losses with a recovery of only 26% (±4.4) of particles and 18% (±1.8) of protein (Table 1). In general, we confirmed previous observations that 10 kDa spinfilters gave higher recovery rates compared to 100 kDa spinfilters . In this study, it was confirmed that EV losses were caused by adhesion of EVs to the filter membranes, as displayed by presence of EV marker proteins in spinfilter membrane lysates [30]. Unexpectedly, 15 ml spinfilters appeared to provide higher recoveries compared to smaller 4 ml spinfilters, despite having larger membrane surface area.

Unfortunately, even with the most optimal 15 ml 10 kDa spinfilters, high EV losses during concentration steps occur. Therefore, alternative EV concentration methods are sought after. Although ultracentrifugation is a widely used alternative method for EV isolation and concentration, functionality of EVs may be harmed during high-speed spins [26]. As an alternative, Zhang et al. [17] suggested PEG precipitation as a method to isolate or concentrate EVs with high recovery rates. In our hands, however, PEG precipitation was ineffective for concentrating pure EVs. In contrast to our approach, Zhang et al. performed PEG precipitation to purify EVs from crude materials which once more suggests that efficiency of EV precipitation using PEG depends on the presence of high concentrations of protein, as described before [31].

Also nonspecific adhesion to the surface of storage containers can influence EV yields, but no clear consensus which materials are optimal for EV storage exist. We therefore assessed storage in different tubes made of polypropene or hydrophilic or hydrophobic glass. Our results indicate that storage in glass tubes gives high EV losses with lower recovery rates of 62% (±3.4) for particles and 68% (±4.0) for proteins compared to storage in regular polypropylene tubes with recovery rates

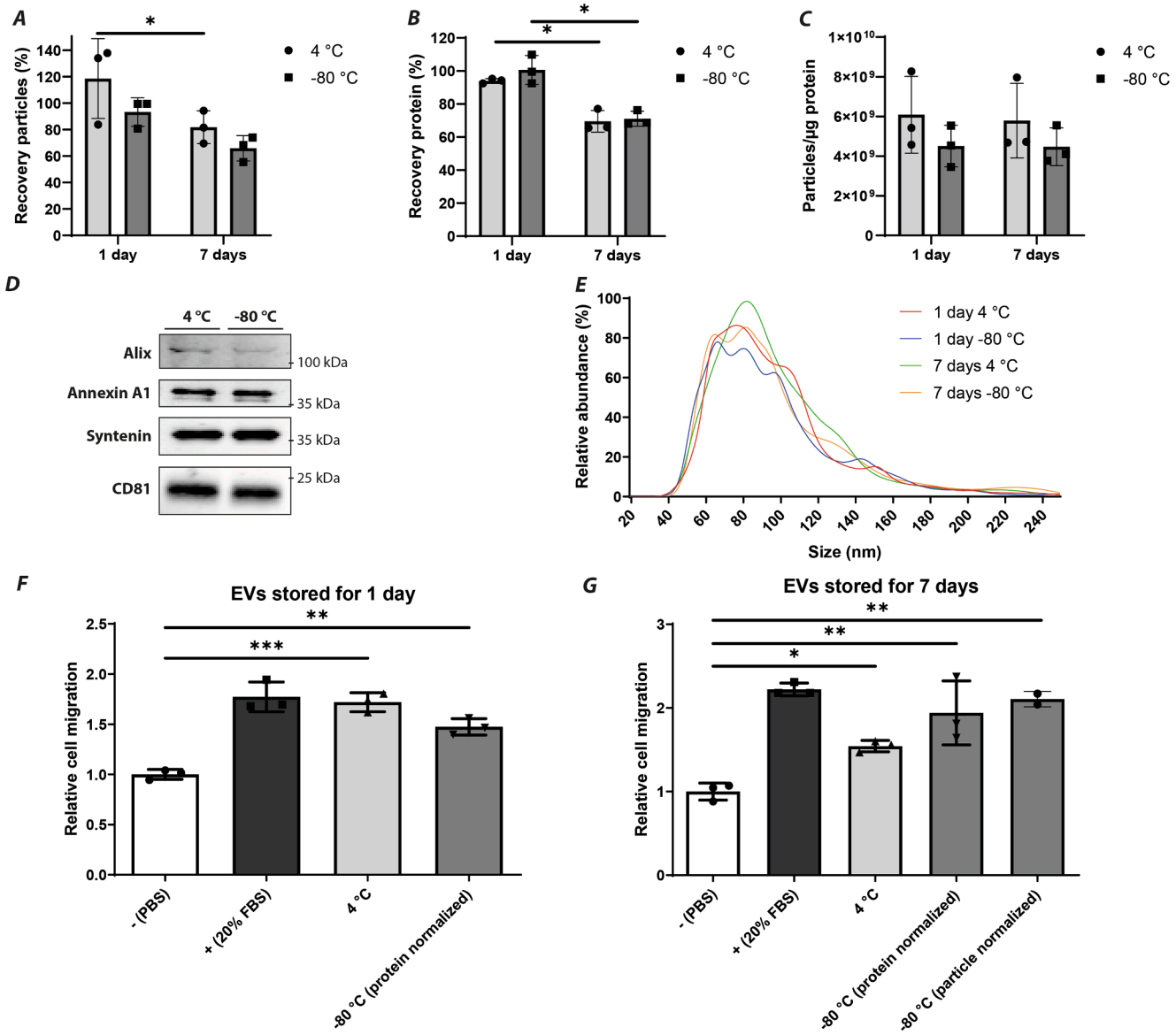

Fig. 7. Effect of different storage temperatures on EV recovery and functionality. A: Particle recovery rates as determined by NTA after 1 and 7 days (Stock: $1.9E^{12} \pm 6.0E^{11}$ particles/ml). **B:** Protein recovery rates as determined by microBCA protein determination after 1 and 7 days (Stock: 405.6 ± 126.8 µg/ml). **C:** Particle/protein ratios of EVs. **D:** Western blot analysis after 7 days of EV storage of the EV marker proteins CD81, syntenin, alix and annexin A1. Equal percentages of the total volume of EV isolates were loaded. **E:** Size ranges of EVs stored at 4 °C and −80 °C. **F:** Results of an endothelial cell wound healing assay performed after 1 day of EV storage. **G:** Results of an endothelial cell wound healing assay performed after 7 days of EV storage. In F, EVs stored at both 4 °C and −80 °C were normalized based on protein quantification only and in G normalization was done both on protein and particle quantification. Results represent biological replicates (n = 3). Significance levels are demonstrated with asterisks (* $p < 0.05$, ** $p < 0.01$, *** $p < 0.001$).

Table 1
Summary of increases in recovery rates for conditions evaluated in this study.

	Particle	Protein
HBS vs PBS	*+ 14.0% ± 6.0*	*− 11.7% ± 11.6*
10 kDa 15 ml vs 100 kDa 4 ml spinfilter	*+ 177.3% ± 30.3*	*+ 192.3% ± 30.0*
10 kDa 15 ml spinfilter vs PEG precipitation	*+ 833.7% ± 134.2*	*+ 1304.0% ± 261.2*
Regular tube vs hydrophilic glass tube	*+ 13.6% ± 15.8*	*+ 14.7% ± 8.7*
0.005% Tween vs no excipient	*+ 26.0% ± 7.8*	*+ 14.9 % ± 3.1*
0.2% BSA vs no excipient	*+ 23.9% ± 6.5*	*N.D.*
4 °C vs −80 °C	*+ 24.1% ± 18.7*	*− 2.2% ± 9.2*

Results represent mean percentage increase ± standard deviation N.D.: not determined.

of 71% (±8.0) for particles and 78% (±4.9) for proteins after 7 days. Our findings are not in line with a different report in which a 32% increased EV recovery was found for low protein binding tubes compared to regular polypropylene tubes [28]. This apparent discrepancy could be the result of differences in EV purity, EV concentration or EV source, and warrant further investigation.

To protect EVs against aggregation and adhesion during storage further, the use of BSA and Tween 20 was explored. BSA is widely used as a stabilizing agent in different pharmaceutical applications [32], and is used to prevent adhesion of other proteins to surfaces, as cosolvent or as cryoprotectant [33]. Tween is a widely used non-ionic surfactant, and is used as solubilizing agent, suspending agent or as wetting agent [33]. Tween is known to be able to cover solid–liquid interfaces and block adhesion of biologicals to tubing, but it can also control the surface charge of EVs which influences the colloidal stability [34]. Here, we

observed that Tween and BSA were both able to reduce EV loss during storage, without impairing EV function (Table 1). Similar results were shown by Evtushenko et al. [28] who observed higher recovery rates in storage tubes after preincubation with BSA. Additionally, BSA may also be employed for pre-equilibration of size exclusion chromatography columns to reduce EV losses during purification [17]. However, as a downside, the use of BSA largely prohibits further EV quantification methods based on total protein content.

Recent studies have suggested that storage temperature impacts EVs' physicochemical characteristics such as size, number, and morphological features [35–37]. However, evaluation of physical parameters of EVs does not predict potential subsequent effects on EV function, which is of obvious importance. Here, EVs stored at both 4 °C and −80 °C displayed decreased particle and protein recoveries over time, with a slightly lower particle recovery for EVs stored at −80 °C compared to 4 °C. A decrease in particle number could be the result of EV adherence to storage tubes, or reduced EV integrity upon rupture during the freeze-thawing process. In published literature, controversy on this topic exists. While some studies show reduced particle numbers exclusively after 4 °C storage [36], others show highest recovery rates at 4 °C [38] or detect no differences between 4 °C and −80 °C storage [35]. Nevertheless, long-term storage, i.e. up to 30 days, at −20 °C and especially −80 °C was reported to be more suited for preservation compared to 4 °C [38,39]. When assessing storage-mediated effects on EV characteristics, we confirmed that average EV sizes remained similar after short-term storage at 4 °C and −80 °C, as compared to freshly isolated EVs [35,36,40]. Conversely, Maroto et al. [37] observed a size shift towards larger EVs, probably caused by swelling, fusion or aggregation of EVs when stored for longer time periods. Park et al. [35], on the other hand, showed that median EV size decreased over time when stored for longer periods at 4 °C and −80 °C.

Our findings further showed preservation of EV function for either tested storage temperature which is supported by previous work [35]. In contrast, the antibacterial capacity of human neutrophilic granulocyte-derived EVs on S. aureus was impaired 1 day after storage at 4 °C compared to fresh EVs [36]. Our results suggest that for short-term storage, both 4 °C and −80 °C storage provide EVs with retained *in vitro* migration functionality, while for long-term storage (a week or longer) −80 °C storage may be preferable.

One limitation of our study is that stability and EV recovery was only evaluated up to one week. Future studies should point out whether our findings also apply to long-term storage. Although the results in this paper were highly reproducible, optimal EV stability and storage may be dependent on the quality and purity of EVs and should be reevaluated for each unique situation. In addition, EVs derived from other sources or obtained via other isolation procedures might favor other conditions or methods for optimized recovery.

Altogether, this study provides insights on which steps are important to optimize to recover appropriate EV yields. Optimization of EV isolation, concentration and storage protocols helps to increase EV recovery and thereby to a lower need for EV production upscaling. Better understanding of protective excipients and buffer formulations on EV function will help EV research to accelerates translation of EV-based therapeutics towards clinical application.

Declaration of Competing Interest

The authors declare that they have no known competing financial interests or personal relationships that could have appeared to influence the work reported in this paper.

Acknowledgements

This work is financially supported by the Van Herk Foundation to SvdW and EVICARE (#725229) of the European Research Council (ERC) to JS. Fig. 1A, 2A, 3A, 4A and the graphical abstract were designed using BioRender (BioRender.com). The authors acknowledge Cor Seinen for excellent technical assistance with TEM. AG is an International Society for Advancement of Cytometry (ISAC) Marylou Ingram Scholar 2019-2023.

Disclosure statement

A.G. and S.E.A. are consultants for and have equity interests in Evox Therapeutics Ltd. P.V. serves on the scientific advisory board of Evox Therapeutics Ltd.

Appendix A. Supplementary material

Supplementary data to this article can be found online at https://doi.org/10.1016/j.ejpb.2021.11.012.

References

[1] S. Gandham, X. Su, J. Wood, A.L. Nocera, S.C. Alli, L. Milane, A. Zimmerman, M. Amiji, A.R. Ivanov, Technologies and Standardization in Research on Extracellular Vesicles, Trends Biotechnol. 38 (10) (2020) 1066–1098.
[2] G. van Niel, G. D'Angelo, G. Raposo, Shedding light on the cell biology of extracellular vesicles, Nat Rev Mol Cell Biol 19 (4) (2018) 213–228.
[3] J.P.G. Sluijter, S.M. Davidson, C.M. Boulanger, E.I. Buzas, D.P.V. De Kleijn, F. B. Engel, Z. Giricz, D.J. Hausenloy, R. Kishore, S. Lecour, J. Leor, Extracellular vesicles in diagnostics and therapy of the ischaemic heart: Position Paper from the Working Group on Cellular Biology of the Heart of the European Society of Cardiology, Cardiovasc. Res. 114 (1) (2018) 19–34.
[4] C. Lässer, Exosomes in diagnostic and therapeutic applications: biomarker, vaccine and RNA interference delivery vehicle, Expert Opin. Biol. Ther. 15 (1) (Jan. 2015) 103–117, https://doi.org/10.1517/14712598.2015.977250.
[5] P. Simeone, G. Bologna, P. Lanuti, L. Pierdomenico, M.T. Guagnano, D. Pieragostino, P. Del Boccio, D. Vergara, M. Marchisio, S. Miscia, R. Mariani-Costantini, Extracellular vesicles as signaling mediators and disease biomarkers across biological barriers, Int. J. Mol. Sci. 21 (7) (2020) 2514.
[6] O.P. Wiklander, M.Á. Brennan, J. Lötvall, X.O. Breakefield, S.E. Andaloussi, Advances in therapeutic applications of extracellular vesicles, Sci. Transl. Med. 11 (492) (2019).
[7] X.-C. Jiang, J.-Q. Gao, Exosomes as novel bio-carriers for gene and drug delivery, Int. J. Pharm. 521 (1–2) (Apr. 2017) 167–175, https://doi.org/10.1016/j.ijpharm.2017.02.038.
[8] S. Dai, D. Wei, Z. Wu, X. Zhou, X. Wei, H. Huang, G. Li, Phase I Clinical Trial of Autologous Ascites-derived Exosomes Combined With GM-CSF for Colorectal Cancer, Mol. Ther. 16 (4) (2008) 782–790.
[9] S. Viaud, S. Ploix, V. Lapierre, C. Théry, P.-H. Commere, D. Tramalloni, K. Gorrichon, P. Virault-Rocroy, T. Tursz, O. Lantz, L. Zitvogel, N. Chaput, Updated technology to produce highly immunogenic dendritic cell-derived exosomes of clinical grade: A critical role of interferon-γ, J. Immunother. 34 (1) (2011) 65–75, https://doi.org/10.1097/CJI.0b013e3181fe535b.
[10] D. Tsiapalis, L. O'Driscoll, Mesenchymal Stem Cell Derived Extracellular Vesicles for Tissue Engineering and Regenerative Medicine Applications, Cells 9 (4) (Apr. 2020) 991, https://doi.org/10.3390/cells9040991.
[11] M.B. Herrera, V. Fonsato, S. Gatti, M.C. Deregibus, A. Sordi, D. Cantarella, R. Calogero, B. Bussolati, C. Tetta, G. Camussi, Human liver stem cell-derived microvesicles accelerate hepatic regeneration in hepatectomized rats, J. Cell Mol. Med. 14 (6b) (2010) 1605–1618.
[12] S. Gatti, S. Bruno, M.C. Deregibus, A. Sordi, V. Cantaluppi, C. Tetta, G. Camussi, Microvesicles derived from human adult mesenchymal stem cells protect against ischaemia–reperfusion-induced acute and chronic kidney injury, Nephrol. Dial. Transplant. 26 (5) (2011) 1474–1483.
[13] F.J. Alibhai, S.W. Tobin, A. Yeganeh, R.D. Weisel, R.-K. Li, Emerging roles of extracellular vesicles in cardiac repair and rejuvenation, American Journal of Physiology-Heart and Circulatory Physiology 315 (4) (2018) H733–H744.
[14] J.A. Maring, K. Lodder, E. Mol, V. Verhage, K.C. Wiesmeijer, C.K.E. Dingenouts, A. T. Moerkamp, J.C. Deddens, P. Vader, A.M. Smits, J.P.G. Sluijter, M.-J. Goumans, Cardiac Progenitor Cell-Derived Extracellular Vesicles Reduce Infarct Size and Associate with Increased Cardiovascular Cell Proliferation, J Cardiovasc. Transl. Res. 12 (1) (2019) 5–17, https://doi.org/10.1007/s12265-018-9842-9.
[15] K.R. Vrijsen, et al., Cardiomyocyte progenitor cell-derived exosomes stimulate migration of endothelial cells, J. Cell. Mol. Med. 14 (5) (2010) 1064–1070.
[16] T. Yamashita, Y. Takahashi, M. Nishikawa, Y. Takakura, Effect of exosome isolation methods on physicochemical properties of exosomes and clearance of exosomes from the blood circulation, Eur. J. Pharm. Biopharm. 98 (Jan. 2016) 1–8, https://doi.org/10.1016/j.ejpb.2015.10.017.
[17] X. Zhang, E.G.F. Borg, A.M. Liaci, H.R. Vos, W. Stoorvogel, A novel three step protocol to isolate extracellular vesicles from plasma or cell culture medium with both high yield and purity, Journal of Extracellular Vesicles 9 (1) (2020) 1791450, https://doi.org/10.1080/20013078.2020.1791450.
[18] A.M. Smits, P. van Vliet, C.H. Metz, T. Korfage, J.PG. Sluijter, P.A. Doevendans, M.-J. Goumans, Human cardiomyocyte progenitor cells differentiate into functional mature cardiomyocytes: an in vitro model for studying human cardiac physiology

and pathophysiology, Nat. Protoc. 4 (2) (2009) 232–243, https://doi.org/10.1038/nprot.2008.229.
[19] A. Görgens, M. Bremer, R. Ferrer-Tur, F. Murke, T. Tertel, P.A. Horn, S. Thalmann, J.A. Welsh, C. Probst, C. Guerin, C.M. Boulanger, J.C. Jones, H. Hanenberg, U. Erdbrügger, J. Lannigan, F.L. Ricklefs, S. El-Andaloussi, B. Giebel, Optimisation of imaging flow cytometry for the analysis of single extracellular vesicles by using fluorescence-tagged vesicles as biological reference material, J. Extracell. Vesicles 8 (1) (2019) 1587567, https://doi.org/10.1080/20013078.2019.1587567.
[20] C. Théry, K.W. Witwer, E. Aikawa, M.J. Alcaraz, J.D. Anderson, R. Andriantsitohaina, A. Antoniou, T. Arab, F. Archer, G.K. Atkin-Smith, D.C. Ayre, J.-M. Bach, D. Bachurski, H. Baharvand, L. Balaj, S. Baldacchino, N.N. Bauer, A. A. Baxter, M. Bebawy, C. Beckham, A. Bedina Zavec, A. Benmoussa, A.C. Berardi, P. Bergese, E. Bielska, C. Blenkiron, S. Bobis-Wozowicz, E. Boilard, W. Boireau, A. Bongiovanni, F.E. Borràs, S. Bosch, C.M. Boulanger, X. Breakefield, A.M. Breglio, M.Á. Brennan, D.R. Brigstock, A. Brisson, M.LD. Broekman, J.F. Bromberg, P. Bryl-Górecka, S. Buch, A.H. Buck, D. Burger, S. Busatto, D. Buschmann, B. Bussolati, E. I. Buzás, J.B. Byrd, G. Camussi, D.RF. Carter, S. Caruso, L.W. Chamley, Y.-T. Chang, C. Chen, S. Chen, L. Cheng, A.R. Chin, A. Clayton, S.P. Clerici, A. Cocks, E. Cocucci, R.J. Coffey, A. Cordeiro-da-Silva, Y. Couch, F.AW. Coumans, B. Coyle, R. Crescitelli, M.F. Criado, C. D'Souza-Schorey, S. Das, A. Datta Chaudhuri, P. de Candia, E.F. De Santana, O. De Wever, H.A. del Portillo, T. Demaret, S. Deville, A. Devitt, B. Dhondt, D. Di Vizio, L.C. Dieterich, V. Dolo, A.P. Dominguez Rubio, M. Dominici, M.R. Dourado, T.AP. Driedonks, F.V. Duarte, H.M. Duncan, R. M. Eichenberger, K. Ekström, S. EL Andaloussi, C. Elie-Caille, U. Erdbrügger, J. M. Falcón-Pérez, F. Fatima, J.E. Fish, M. Flores-Bellver, A. Försönits, A. Frelet-Barrand, F. Fricke, G. Fuhrmann, S. Gabrielsson, A. Gámez-Valero, C. Gardiner, K. Gärtner, R. Gaudin, Y.S. Gho, B. Giebel, C. Gilbert, M. Gimona, I. Giusti, D. CI. Goberdhan, A. Görgens, S.M. Gorski, D.W. Greening, J.C. Gross, A. Gualerzi, G. N. Gupta, D. Gustafson, A. Handberg, R.A. Haraszti, P. Harrison, H. Hegyesi, A. n. Hendrix, A.F. Hill, F.H. Hochberg, K.F. Hoffmann, B. Holder, H. Holthofer, B. Hosseinkhani, G. Hu, Y. Huang, V. Huber, S. Hunt, A.-E. Ibrahim, T. Ikezu, J. M. Inal, M. Isin, A. Ivanova, H.K. Jackson, S. Jacobsen, S.M. Jay, M. Jayachandran, G. Jenster, L. Jiang, S.M. Johnson, J.C. Jones, A. Jong, T. Jovanovic-Talisman, S. Jung, R. Kalluri, S.-I. Kano, S. Kaur, Y. Kawamura, E.T. Keller, D. Khamari, E. Khomyakova, A. Khvorova, P. Kierulf, K.P. Kim, T. Kislinger, M. Klingeborn, D. J. Klinke, M. Kornek, M.M. Kosanović, Á.F. Kovács, E.-M. Krämer-Albers, S. Krasemann, M. Krause, I.V. Kurochkin, G.D. Kusuma, S. Kuypers, S. Laitinen, S. M. Langevin, L.R. Languino, J. Lannigan, C. Lässer, L.C. Laurent, G. Lavieu, E. Lázaro-Ibáñez, S. Le Lay, M.-S. Lee, Y.X.F. Lee, D.S. Lemos, M. Lenassi, A. Leszczynska, I.TS. Li, K.e. Liao, S.F. Libregts, E. Ligeti, R. Lim, S.K. Lim, A. Linē, K. Linnemannstöns, A. Llorente, C.A. Lombard, M.J. Lorenowicz, Á.M. Lörincz, J. Lötvall, J. Lovett, M.C. Lowry, X. Loyer, Q. Lu, B. Lukomska, T.R. Lunavat, S. LN. Maas, H. Malhi, A. Marcilla, J. Mariani, J. Mariscal, E.S. Martens-Uzunova, L. Martin-Jaular, M.C. Martinez, V.R. Martins, M. Mathieu, S. Mathivanan, M. Maugeri, L.K. McGinnis, M.J. McVey, D.G. Meckes, K.L. Meehan, I. Mertens, V. R. Minciacchi, A. Möller, M. Møller Jørgensen, A. Morales-Kastresana, J. Morhayim, F. Mullier, M. Muraca, L. Musante, V. Mussack, D.C. Muth, K. H. Myburgh, T. Najrana, M. Nawaz, I. Nazarenko, P. Nejsum, C. Neri, T. Neri, R. Nieuwland, L. Nimrichter, J.P. Nolan, E.NM. Nolte-'t Hoen, N. Noren Hooten, L. O'Driscoll, T. O'Grady, A. O'Loghlen, T. Ochiya, M. Olivier, A. Ortiz, L.A. Ortiz, X. Osteikoetxea, O. Østergaard, M. Ostrowski, J. Park, D.M. Pegtel, H. Peinado, F. Perut, M.W. Pfaffl, D.G. Phinney, B.CH. Pieters, R.C. Pink, D.S. Pisetsky, E. Pogge von Strandmann, I. Polakovicova, I.KH. Poon, B.H. Powell, I. Prada, L. Pulliam, P. Quesenberry, A. Radeghieri, R.L. Raffai, S. Raimondo, J. Rak, M.I. Ramirez, G. Raposo, M.S. Rayyan, N. Regev-Rudzki, F.L. Ricklefs, P.D. Robbins, D. D. Roberts, S.C. Rodrigues, E. Rohde, S. Rome, K.MA. Rouschop, A. Rughetti, A. E. Russell, P. Saá, S. Sahoo, E. Salas-Huenuleo, C. Sánchez, J.A. Saugstad, M. J. Saul, R.M. Schiffelers, R. Schneider, T.H. Schøyen, A. Scott, E. Shahaj, S. Sharma, O. Shatnyeva, F. Shekari, G.V. Shelke, A.K. Shetty, K. Shiba, P.-M. Siljander, A. M. Silva, A. Skowronek, O.L. Snyder, R.P. Soares, B.W. Sódar, C. Soekmadji, J. Sotillo, P.D. Stahl, W. Stoorvogel, S.L. Stott, E.F. Strasser, S. Swift, H. Tahara, M. Tewari, K. Timms, S. Tiwari, R. Tixeira, M. Tkach, W.S. Toh, R. Tomasini, A. C. Torrecilhas, J.P. Tosar, V. Toxavidis, L. Urbanelli, P. Vader, B.WM. van Balkom, S.G. van der Grein, J. Van Deun, M.JC. van Herwijnen, K. Van Keuren-Jensen, G. van Niel, M.E. van Royen, A.J. van Wijnen, M.H. Vasconcelos, I.J. Vechetti, T. D. Veit, L.J. Vella, É. Velot, F.J. Verweij, B. Vestad, J.L. Viñas, T. Visnovitz, K. V. Vukman, J. Wahlgren, D.C. Watson, M.HM. Wauben, A. Weaver, J.P. Webber, V. Weber, A.M. Wehman, D.J. Weiss, J.A. Welsh, S. Wendt, A.M. Wheelock, Z. Wiener, L. Witte, J. Wolfram, A. Xagorari, P. Xander, J. Xu, X. Yan, M. Yáñez-Mó, H. Yin, Y. Yuana, V. Zappulli, J. Zarubova, V. Žėkas, J.-y. Zhang, Z. Zhao, L. Zheng, A.R. Zheutlin, A.M. Zickler, P. Zimmermann, A.M. Zivkovic, D. Zocco, E. K. Zuba-Surma, (MISEV2018): a position statement of the International Society for Extracellular Vesicles and update of the MISEV2014 guidelines", J. Extracell. Vesicles 7 (1) (2018) 1535750, https://doi.org/10.1080/20013078.2018.1535750.
[21] "Common buffers, media, and stock solutions," *Curr. Protoc. Hum. Genet.*, vol. Appendix 2, p. Appendix 2D, May 2001, doi: 10.1002/0471142905.hga02ds26.
[22] P. Kolhe, E. Amend, S. K. Singh, Impact of freezing on pH of buffered solutions and consequences for monoclonal antibody aggregation, Biotechnol. Prog. 26 (3) (2010) 727–733, https://doi.org/10.1002/btpr.377.
[23] M.M. Bahr, M.S. Amer, K. Abo-El-Sooud, A.N. Abdallah, O.S. El-Tookhy, Preservation techniques of stem cells extracellular vesicles: a gate for manufacturing of clinical grade therapeutic extracellular vesicles and long-term clinical trials, Int. J. Vet. Sci. Med. 8 (1) (2020) 1–8, https://doi.org/10.1080/23144599.2019.1704992.
[24] A. Sheikhi, S. Afewerki, R. Oklu, A.K. Gaharwar, A. Khademhosseini, Effect of ionic strength on shear-thinning nanoclay-polymer composite hydrogels, Biomater. Sci. 6 (8) (Jul. 2018) 2073–2083, https://doi.org/10.1039/c8bm00469b.
[25] J. Webber, A. Clayton, How pure are your vesicles? J. Extracell. Vesicles 2 (1) (2013) 1–6, https://doi.org/10.3402/jev.v2i0.19861.
[26] E.A. Mol, M.J. Goumans, P.A. Doevendans, J.P.G. Sluijter, P. Vader, Higher functionality of extracellular vesicles isolated using size-exclusion chromatography compared to ultracentrifugation, Nanomedicine Nanotechnol. Biol. Med. 13 (6) (2017) 2061–2065.
[27] K.R. Vrijsen, et al., Exosomes from Cardiomyocyte Progenitor Cells and Mesenchymal Stem Cells Stimulate Angiogenesis Via EMMPRIN, Adv. Healthc. Mater. 5 (19) (2016) 2555–2565.
[28] E.G. Evtushenko, D.V. Bagrov, V.N. Lazarev, M.A. Livshits, E. Khomyakova, J. Chalmers, Adsorption of extracellular vesicles onto the tube walls during storage in solution, PLoS ONE 15 (12) (Dec. 2020) e0243738, https://doi.org/10.1371/journal.pone.0243738.
[29] A. Kratzer, F. Kees, C. Dorn, Unbound fraction of fluconazole and linezolid in human plasma as determined by ultrafiltration: Impact of membrane type, J. Chromatogr. B 1039 (Dec. 2016) 74–78, https://doi.org/10.1016/j.jchromb.2016.10.040.
[30] G. Vergauwen, B. Dhondt, J. Van Deun, E. De Smedt, G. Berx, E. Timmerman, K. Gevaert, I. Miinalainen, V. Cocquyt, G. Braems, R. Van den Broecke, H. Denys, O. De Wever, A.n. Hendrix, Confounding factors of ultrafiltration and protein analysis in extracellular vesicle research, Sci. Rep. 7 (1) (2017), https://doi.org/10.1038/s41598-017-02599-y.
[31] K.C. Ingham, "[20] Protein precipitation with polyethylene glycol", in *Methods in Enzymology* vol. 104 (1984) 351–356.
[32] K.A. Majorek, P.J. Porebski, A. Dayal, M.D. Zimmerman, K. Jablonska, A. J. Stewart, M. Chruszcz, W. Minor, Structural and immunologic characterization of bovine, horse, and rabbit serum albumins, Mol. Immunol. 52 (3-4) (2012) 174–182, https://doi.org/10.1016/j.molimm.2012.05.011.
[33] Z. Kanzaki, "Handbook-of-Pharmaceutical-Excipients 6th Edition", Accessed: Jul. 21, 2021. [Online]. Available: https://www.academia.edu/16731682/Handbook_of_Pharmaceutical_Excipients_6th_Edition.
[34] G. Midekessa, K. Godakumara, J. Ord, J. Viil, F. Lättekivi, K. Dissanayake, S. Kopanchuk, A. Rinken, A. Andronowska, S. Bhattacharjee, T. Rinken, A. Fazeli, Zeta Potential of Extracellular Vesicles: Toward Understanding the Attributes that Determine Colloidal Stability, ACS Omega 5 (27) (2020) 16701–16710, https://doi.org/10.1021/acsomega.0c01582.
[35] S.J. Park, H. Jeon, S.-M. Yoo, M.-S. Lee, The effect of storage temperature on the biological activity of extracellular vesicles for the complement system, In Vitro Cell. Dev. Biol. Anim. 54 (6) (2018) 423–429.
[36] Á.M. Lőrincz, et al., Effect of storage on physical and functional properties of extracellular vesicles derived from neutrophilic granulocytes, J. Extracell. Vesicles 3 (2014) 25465.
[37] R. Maroto, Y. Zhao, M. Jamaluddin, V.L. Popov, H. Wang, M. Kalubowilage, Y. Zhang, J. Luisi, H. Sun, C.T. Culbertson, S.H. Bossmann, M. Motamedi, A. R. Brasier, Effects of storage temperature on airway exosome integrity for diagnostic and functional analyses, J. Extracell. Vesicles 6 (1) (2017) 1359478, https://doi.org/10.1080/20013078.2017.1359478.
[38] Y. Cheng, Q. Zeng, Q. Han, W. Xia, Effect of pH, temperature and freezing-thawing on quantity changes and cellular uptake of exosomes, Protein Cell 10 (4) (Apr. 2019) 295–299, https://doi.org/10.1007/s13238-018-0529-4.
[39] M. Lee, J.-J. Ban, W. Im, M. Kim, Influence of storage condition on exosome recovery, Biotechnol. Bioprocess Eng. 21 (2) (Mar. 2016) 299–304, https://doi.org/10.1007/s12257-015-0781-x.
[40] V. Sokolova, A.-K. Ludwig, S. Hornung, O. Rotan, P.A. Horn, M. Epple, B. Giebel, Characterisation of exosomes derived from human cells by nanoparticle tracking analysis and scanning electron microscopy, Colloids Surf. B Biointerfaces 87 (1) (2011) 146–150, https://doi.org/10.1016/j.colsurfb.2011.05.013.